

Generalized hydrodynamic analysis of transport through a finite open nanopore for two-component single-file systems

King C. Lai ^{1,2} Tyler J. Pleasant ¹ Andrés García,¹ and James W. Evans ^{1,2,3}

¹*Ames Laboratory—USDOE, Iowa State University, Ames, Iowa 50011, USA*

²*Department of Physics & Astronomy, Iowa State University, Ames, Iowa 50011, USA*

³*Department of Mathematics, Iowa State University, Ames, Iowa 50011, USA*



(Received 15 February 2020; revised manuscript received 6 April 2020; accepted 28 April 2020; published 1 June 2020)

Single-file diffusion (SFD) in finite open nanopores is characterized by nonzero spatially varying tracer diffusion coefficients within a generalized hydrodynamic description. This contrasts with infinite SFD systems where tracer diffusivity vanishes. In standard tracer counterpermeation (TCP) analysis, two reservoirs, each containing a different species, are connected to opposite ends of a finite pore. We implement an *extended TCP analysis* to allow the two reservoirs to contain slightly different mixtures of the two species. Then, determination of diffusion fluxes through the pore allows extraction of diffusion coefficients for near-constant partial concentrations of the two species. This analysis is applied for a lattice-gas model describing two-component SFD through a finite linear pore represented by a one-dimensional array of cells. Two types of particles, A and B, can hop only to adjacent empty cells with generally different rates, h_A and h_B . Particles are noninteracting other than exclusion of multiple cell occupancy. Results reveal generalized hydrodynamic tracer diffusion coefficients which adopt small values inversely proportional to pore length in the pore center, but which are strongly enhanced near pore openings.

DOI: [10.1103/PhysRevE.101.062103](https://doi.org/10.1103/PhysRevE.101.062103)

I. INTRODUCTION

Inhibited diffusive transport through finite-length nanopores with ends open to fluid reservoirs is of direct relevance to several applications. These include transport across biological membranes [1–3], as well as separations [4–7] and catalysis [8–11] utilizing inorganic nanoporous materials. An extreme case of inhibited transport corresponds to single-file diffusion (SFD) [12–15] where species cannot pass each other inside the pore. Significantly, early studies of biological transport recognized the potential of anomalous behavior in this single-file diffusion (SFD) regime [3]. Separations involve competitive transport of two or more species, often through nanoporous membranes. These processes naturally relate to the current study which considers transport for two species with different mobilities subject to SFD. Often differences in the strength of adsorption for different species is a key component of separation efficiency [4,6], but our study is more relevant to separations of nonadsorbing species. For applications to catalysis in nanoporous systems [8–11], again at least two distinct species diffuse in the pore, i.e., reactants and products. However, the relevance of an analysis of transport in the absence of reaction, as studied here, to the description of catalytic reaction-diffusion processes deserves further comment which we now provide.

In this context, first consider the treatment of reaction-diffusion processes in the hydrodynamic regime [16–18] where diffusion rates far exceed reaction rates. In this regime, spatial concentration gradients are small and the kinetics is

reaction limited. Then, analysis of transport in the absence of reaction is performed, and the generally nontrivial results provide input to the hydrodynamic reaction-diffusion equations describing exactly the reactive system. This approach has been applied effectively, e.g., for low-pressure catalytic reactions on single-crystal surfaces, to generate a precise beyond-mean-field analysis of spatiotemporal reaction-diffusion phenomena [11,18,19]. However, of more relevance here is the analysis of catalytic conversion reactions in linear nanopores with inhibited transport, including the SFD regime where reactant and product species cannot pass each other [20–23]. Such systems cannot be regarded as corresponding to the hydrodynamic regime given their finite size (on the order of 100 nm), and due to large concentration gradients. Also, traditional mean-field reaction-diffusion equation treatments fail dramatically to capture the behavior of the subtle interplay between inhibited transport and reaction [23]. Yet the above strategy of first analyzing the nontrivial transport properties of the corresponding nonreactive system, and then incorporating results in a description of reaction kinetics, has proved to be highly successful in capturing nontrivial non-mean-field reactivity behavior [11,23]. This type of so-called generalized hydrodynamic treatment is actually more common in a conventional fluid mechanics context [24].

It is appropriate to recall that Onsager theory provides a precise treatment of transport for single- and multicomponent systems, but only in the above-mentioned hydrodynamic regime of large length scales and small concentration gradients [16,25]. Consequently, this theoretical framework is not directly applicable to the finite open systems of interest

in this study. However, it does provide some insights into the appropriate generalized hydrodynamic treatment [23,24] which will prove effective for describing behavior on the relevant shorter length scales, as well as incorporating pore end effects [11,23]. In addition, for the systems of interest here with a SFD constraint, it is natural to investigate any resultant simplifying features of the general Onsager theory which are imposed by this constraint.

Another perspective on the challenge of describing transport in finite SFD systems comes from precise theoretical and simulation studies of tracer diffusion in finite closed systems with periodic boundary conditions. Such studies have been applied to treat single-component SFD systems providing insight into the particle concentration dependence of the tracer diffusion coefficient, and also revealing an inverse proportionality to pore length [26,27]. (In such analyses, there is a need to define displacement of the tagged particle so that it can increase without bound.) The dependence on pore length is consistent with the classic result for SFD that the tracer diffusion coefficient vanishes in an infinite system due to a sublinear increase in the mean-square displacement [12]. Various refined analyses have been applied to open finite open systems indicating that some basic features of behavior for periodic systems are preserved including the inverse dependence on pore length [27–29].

However, the approach on which we focus here, and which is targeted to finite open systems, is tracer counterpermeation (TCP) analysis [30,31]. In the standard TCP analysis, two reservoirs each containing the same concentration of differently labeled or “colored” but otherwise identical species are connected to opposite open ends of a finite pore. We emphasize that the two differently colored species have identical mobilities and interactions. After a transient filling period for an initially empty pore, a steady state develops. Determination of the corresponding steady-state fluxes of the two species in opposite directions through the pore allows extraction of a tracer-type diffusion coefficient. This can be regarded as a generalized hydrodynamic tracer diffusion coefficient not just because it applies for a finite-size system (rather than an infinite system), but also because it captures pore end effects (i.e., enhancement of diffusivity near the openings) [30,31]. This latter feature has been shown critical in determining concentration distributions and reaction yield for catalytic conversion reactions in single-file nanopores for the special case of equal reactant and product mobility [11,23].

The natural goal pursued in this contribution is to extend the above TCP studies to treat two species with different mobilities, as is invariably the case for multicomponent separations or for distinct reactant and product species in catalytic conversion reactions. In addition, we will implement an *extended TCP analysis* where each of the two reservoirs connected to opposite ends of the pore no longer includes just a single component (as in the standard TCP analysis). Rather, we allow the reservoirs to include slightly different mixtures of the two components. Then, determination of diffusion fluxes through the pore allows extraction of generalized hydrodynamic tracer diffusion coefficients including for the case of near-constant partial concentrations of the two species.

Finally, we remark that given the complexities of treating transport in multicomponent single-file systems, we naturally

simplify the analysis by considering noninteracting systems (in the sense that the only interaction is the exclusion of passing of particles in the single-file system). This leads to a fundamental simplification in the description of chemical diffusion coefficients for single-component systems [32]. For multicomponent systems of interest here, it greatly simplifies description of system thermodynamics which controls one of two factors determining of chemical diffusion coefficients [11,16,19]. Particularly significant, for the special case of equal mobility in noninteracting two-component systems, is that exact results are available for Onsager diffusion tensor [11,16,33]. These results will provide a touchstone for our treatment of the general case of unequal mobility.

In Sec. II, we describe our stochastic lattice-gas model for the two-component single-file system, as well as the associated master equations. Standard and generalized hydrodynamic theories for the above model are presented in Sec. III. Results from kinetic Monte Carlo simulation analysis of the model are presented in Sec. IV, and additional discussion is provided in Sec. V. Conclusions are reported in Sec. VI.

II. LATTICE-GAS MODEL AND HETEROGENEOUS MASTER EQUATIONS

A. Lattice-gas model prescription

We consider a stochastic lattice-gas (LG) model describing two-component single-file diffusion through a finite pore. See Fig. 1. The pore is represented by a one-dimensional linear array of sites or cells. The cell width is denoted by a which is usually set to unity. There are two types of particles, A and B, which can hop only to adjacent empty cells with generally different rates, h_A and h_B , respectively. Consequently, this dynamics automatically enforces a SFD constraint. Implicitly, this prescription of dynamics implies that there are no interactions between particles other than the exclusion of occupancy of sites or cells by more than one particle. The above description completely specifies the model for an infinite system, or for a finite system with periodic boundary conditions.

For a finite system with open boundaries of relevance for TCP analysis, the form of coupling between the pore and the reservoirs must also be specified. In this analysis, reservoirs at opposite ends of the pore are not coupled directly, but only coupled through the pore. One approach is to assume that each reservoir corresponds to well-stirred infinite three-dimensional 3D lattice-gas of particles with specified concentration. There is one exterior cell in each reservoir adjacent to an interior end site or cell within the pore. Transport between the reservoir and the pore occurs by particle hopping between these two sites with the same rates as within the pore. Specifically, adsorption of A (B) from exterior cell to the interior end pore cell occurs at rate h_A (h_B) if the interior cell is empty. Desorption of A (B) from an occupied interior end pore cell to the exterior cell occurs at rate h_A (h_B) if the exterior cell is empty. The well-stirred condition for the reservoirs means that there are no spatial correlations within the reservoirs, and that the probability that any reservoir site is occupied by species A or B corresponds to the specified global reservoir

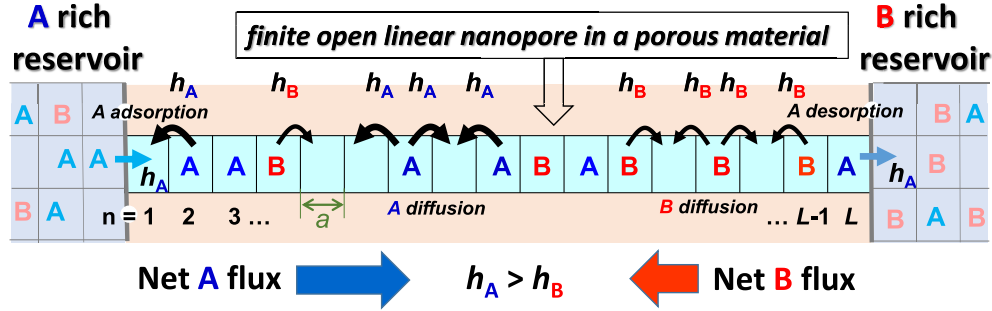


FIG. 1. Schematic of the extended TCP setup for our LG model of a two-component SFD system in a finite open nanopore. Particles A and B hop with rates h_A and h_B , respectively, to adjacent empty cells in the pore which imposes a SFD constraint. Adsorption from and desorption to external reservoirs involve hopping between the interior end pore cell and the adjacent exterior reservoir cell also with rates h_A and h_B . Reservoirs are well stirred.

concentration for that species. This probability impacts the rate of transport into and out of the pore.

For an infinite system or finite pore with periodic boundary conditions, the lack of interactions between particles in the model implies that there are no correlations in the equilibrium state within the pore. This in turn allows simple exact determination of compressibilities based on fluctuation-correlation relations [34,35], the results of which will be utilized in Sec. III.

B. Heterogeneous master equations

Behavior in the above model is described exactly by heterogeneous master equations which can instructively be written in hierarchical form [11]. Let integer n denote the site or cell label, and let $\langle A_n \rangle$ and $\langle B_n \rangle$ denote the probability to find A and B in cell n (i.e., the partial concentrations). Let X (or E) denote the state where the cell is occupied by either type of particle (or unoccupied). Then, one has $\langle X_n \rangle = \langle A_n \rangle + \langle B_n \rangle$ and $\langle X_n \rangle + \langle E_n \rangle = 1$. Let $\langle A_n E_{n+1} \rangle$ denote the probability that cell n is occupied by A and cell $n + 1$ is E, etc. Also let $\nabla \langle C_n \rangle = \langle C_n \rangle - \langle C_{n-1} \rangle$ denote a discrete derivative. Then, except near pore openings, model behavior is described by

$$d/dt \langle A_n \rangle = -\nabla J_A(n) \text{ and } d/dt \langle B_n \rangle = -\nabla J_B(n), \quad (1)$$

with net fluxes $J_{A,B}(n)$ from cell n to cell $n + 1$ given by

$$J_A = h_A[\langle A_n E_{n+1} \rangle - \langle E_n A_{n+1} \rangle] \text{ and } J_B = h_B[\langle B_n E_{n+1} \rangle - \langle E_n B_{n+1} \rangle]. \quad (2)$$

Separate equations apply for the cells at the ends of the pore reflecting the prescription of adsorption and desorption at pore openings described in Sec. II A. These serve as “boundary conditions.” The fluxes (2), which reflect the feature that hopping occurs only to neighboring empty cells, cannot be written in terms of single-cell concentrations due to spatial correlations between occupancy of different cells [11,20–23,36]. Thus (1) is not closed, but rather is just the lowest-order equation in a hierarchy [11]. The next-order equation for pair probabilities involves triplet probabilities. Triplets couple to quartets, etc.

One strategy for model analysis is to implement hierarchical truncation approximations. The lowest-order mean-field

or site approximation neglects all spatial correlations, and obtains a closed set of equations for single-site quantities. The pair approximation writes triplets in terms of pair and single-site quantities, and thus obtains closed coupled equations for single-site and pair quantities. The triplet approximation writes quartets in terms of triplets, etc. However, even these higher-order truncation approximations fail to accurately capture behavior given the strong correlations induced by the SFD constraint [11,36]. See the Appendix for a more detailed discussion, and also the Supplemental Material [37] for additional results.

It is, however, possible to derive an exact relation between the above fluxes by considering the combination

$$J_A/h_A + J_B/h_B = \langle X_n E_{n+1} \rangle - \langle E_n X_{n+1} \rangle = \langle X_n \rangle - \langle X_{n+1} \rangle. \quad (3)$$

The latter reduction utilizes exact relations such as $\langle X_n E_{n+1} \rangle + \langle X_n X_{n+1} \rangle = \langle X_n \rangle$. An analogous reduction has been used in the analysis of the simpler case of transport in single-component systems [32].

In a standard TCP analysis for a finite open pore, the reservoir coupled to one end contains only A with concentration $\langle A \rangle = \langle X \rangle$, and the reservoir at the other end contains only B with the same concentration $\langle B \rangle = \langle X \rangle$. In our extended TCP, we will allow reservoirs to contain different mixtures of A and B, but will maintain the constraint that the total concentration in both reservoirs is the same, $\langle X \rangle$. One could consider even more general situations where the concentrations in the two reservoirs differ. In the latter most general case, in the steady state where fluxes are constant in time and space, (3) implies that the total concentration $\langle X_n \rangle$ varies linearly across the pore. In the standard TCP analysis or in our extension where both reservoirs have the same total concentration $\langle X \rangle$, then (3) implies that $\langle X_n \rangle = \langle X \rangle$ is constant in the pore, and furthermore yields the key result

$$J_A/h_A = -J_B/h_B \text{ (same } \langle X \rangle \text{ for both reservoirs)}. \quad (4)$$

The relation (3) applies more generally for infinite systems or finite systems with periodic boundary systems, but in the equilibrium state of such systems trivially $J_A = J_B = 0$ and $\langle X_n \rangle$ is constant.

III. STANDARD AND GENERALIZED HYDRODYNAMIC THEORIES

A. Onsager hydrodynamic transport analysis

For a comprehensive analysis of our two-component LG model with SFD, it is appropriate to consider a hydrodynamic treatment of transport with and without SFD which applies for macroscopic or infinite systems in the regime of small concentration gradients. This consideration will help guide the subsequent development of a generalized hydrodynamic treatment for the finite open systems of interest here.

First, we comment on the single-component LG model with hopping to nearest-neighbor (NN) empty sites at rate h . (This corresponds to the limit of our two-component model where the concentration of either A or B vanishes.) Exact analysis [32] reveals that the chemical or collective diffusion coefficient is independent of particle concentration, $\langle X \rangle$, and is simply given in terms of the particle hop rate by $D_0 = a^2 h$ where again a denotes the lattice constant (or cell width). For a general LG model, the tracer diffusion coefficient has the form $D_{\text{tr}} = D_0(1 - \langle X \rangle)f(\langle X \rangle)$ where $f \leq 1$ is a correlation factor reflecting back-correlations in the walk of the tagged particle [38]. However, for SFD in infinite systems, one has that $f \equiv 0$ so that $D_{\text{tr}} = 0$.

For a two-component system with species $C = A$ or B , Onsager hydrodynamic transport theory determines species diffusion fluxes, J_C , in terms of gradients in either chemical potentials, μ_C , or densities (i.e., concentrations), $\langle C \rangle$. These fluxes have the form [11,16]

$$J_A = -\Lambda_{AA}\nabla\mu_A - \Lambda_{AB}\nabla\mu_B = -D_{AA}\nabla\langle A \rangle - D_{AB}\nabla\langle B \rangle, \quad (5)$$

with an analogous expression for J_B . The Λ denote Onsager conductivity coefficients and the D denote chemical diffusion coefficients. Collecting these coefficients into a 2×2 asymmetric diffusion tensor, \mathbf{D} , and a symmetric 2×2 conductivity tensor, $\mathbf{\Lambda}$, one obtains the relation $\mathbf{D} = \mathbf{\Lambda} \times \chi^{-1}$ involving the 2×2 symmetric compressibility tensor χ . The components of χ have the form $\chi_{CD} = \partial\langle C \rangle / \partial\mu_D$. For our two-component non-noninteracting LG model, application of fluctuation-dissipation relations immediately shows that [11,16]

$$\chi_{AA} = (k_B T)^{-1}(1 - \langle A \rangle)\langle A \rangle, \quad \chi_{BB} = (k_B T)^{-1}(1 - \langle B \rangle)\langle B \rangle, \quad \text{and}$$

$$\chi_{AB} = \chi_{BA} = (k_B T)^{-1}\langle A \rangle\langle B \rangle, \quad (6)$$

where k_B denotes the Boltzmann constant and T denotes the system temperature.

In the hydrodynamic limit for multicomponent SFD systems, the tracer diffusion coefficient vanishes for any choice of mobilities of the components. However, the chemical diffusion coefficients do not vanish, and are determined for our two-component LG SFD model by first evaluating the Onsager conductivity coefficients. This analysis utilizes the feature that Λ_{CD} measures the diffusion flux of C induced by imposing a bias in the diffusion of species D . For SFD, it is clear that imposing a bias in the diffusion of one species imposes the same flux per particle for all species. Consequently, the induced flux for each species is exactly proportional to the

concentration of that species. As a result, one has

$$\Lambda_{AA}/\Lambda_{BA} = \langle A \rangle / \langle B \rangle \quad \text{and} \quad \Lambda_{BB}/\Lambda_{AB} = \langle B \rangle / \langle A \rangle \quad (\text{for SFD}). \quad (7)$$

Then since $\Lambda_{AB} = \Lambda_{BA}$, (7) implies that all three distinct conductivity coefficients are determined by any one of these, e.g., Λ_{AB} . Using the relationship between \mathbf{D} and $\mathbf{\Lambda}$, an immediate consequence of (6) and (7) is that

$$D_{AA} = D_{AB} = (k_B T)\Lambda_{AB}/(\langle B \rangle\langle E \rangle), \quad (8)$$

$$\text{so that } J_A = -D_{AA}\nabla\langle X \rangle,$$

and

$$D_{BB} = D_{BA} = (k_B T)\Lambda_{AB}/(\langle A \rangle\langle E \rangle), \quad \text{so that} \\ J_B = -D_{BB}\nabla\langle X \rangle = (\langle B \rangle / \langle A \rangle)J_A, \quad (9)$$

where $\langle E \rangle = 1 - \langle A \rangle - \langle B \rangle$. The relationship between J_A and J_B is a direct and natural consequence of SFD.

Complete determination of chemical diffusion coefficients and fluxes requires an additional relation for conductivity coefficients. For noninteracting two-component LG models, this relation has the form [39]

$$\Lambda_{AA}/D_0(A) + \Lambda_{AB}/D_0(B) = (k_B T)^{-1}\langle A \rangle\langle E \rangle, \quad (10)$$

where $D_0(A) = a^2 h_A$ and $D_0(B) = a^2 h_B$. This leads to the explicit results for hydrodynamic diffusion coefficients:

$$D_{AA} = D_0(A)D_0(B)\langle A \rangle / [D_0(B)\langle A \rangle + D_0(A)\langle B \rangle] \quad \text{and} \\ \langle A \rangle D_{BB} = \langle B \rangle D_{AA}. \quad (11)$$

The relations (11) in turn lead to explicit results for hydrodynamic diffusion fluxes J_A and J_B using (8) and (9). Intuitive limiting behavior is also recovered. For example, one has $D_{AA} \sim D_0(B)\langle A \rangle / \langle B \rangle$, as $D_0(A)/D_0(B) \rightarrow \infty$ where slow B diffusivity must control behavior, and also as $\langle A \rangle \rightarrow 0$.

B. Generalized hydrodynamic formulation

The above results show that when the total concentration, $\langle X \rangle$, is constant (as is the case for TCP and extended TCP configurations), then the diffusion fluxes J_A and J_B vanish in the hydrodynamic regime. However, for TCP-type analysis in finite open systems, it is clear from Sec. II that there are nonzero diffusion fluxes through the pore. These fluxes and the associated diffusion coefficients are then naturally characterized as *generalized hydrodynamic* quantities as they reflect both finite-size and pore end effects. Some insight into development of an appropriate formalism is provided by consideration of more general noninteracting LG models still with two components, A and B, hopping to neighboring empty sites or cells with *equal hop rates*, $h_A = h_B = h$, but now also allowing possible exchange of A and B on adjacent sites or cells. In this case, an exact Onsager-based analysis of transport yields the result [16,33]

$$J_A = -D_0(\langle A \rangle / \langle X \rangle)\nabla\langle X \rangle - D_{\text{tr}}[(\langle B \rangle / \langle X \rangle)\nabla\langle A \rangle \\ - (\langle A \rangle / \langle X \rangle)\nabla\langle B \rangle], \quad (12)$$

for $h_A = h_B$ where again $D_0 = a^2 h$, and where D_{tr} is the unique tracer diffusion coefficient (since both A and B have

the same hopping dynamics) which depends on the extent of exchange and on $\langle X \rangle$. An analogous relation describes J_B . For SFD (in the absence of exchange of A and B), D_{tr} vanishes in the hydrodynamic limit and (12) recovers the result (11) in the case where $D_0(A) = D_0(B) = D_0$. However, of more significance here is the observation that for the more general LG model with possible exchange, in the case of constant $\langle X \rangle$ (as applies for the so-called counterdiffusion mode of TCP-type configurations where $\nabla(A) = -\nabla(B)$), (12) reduces to [11,16,23,30]

$$\begin{aligned} J_A &= -D_{tr}\nabla\langle A \rangle \quad \text{and} \\ J_B &= -D_{tr}\nabla\langle B \rangle (= -J_A), \quad \text{for } h_A = h_B. \end{aligned} \quad (13)$$

It is natural to use (13) to define generalized tracer diffusion coefficients for finite systems with $h_A = h_B$, where the fluxes are determined from a TCP-type analysis via [11,30,31]

$$D_{tr}(\text{TCP}) \equiv -J_A/\nabla\langle A \rangle \equiv -J_B/\nabla\langle B \rangle \quad (\text{for } h_A = h_B). \quad (14)$$

This definition has been shown to account for finite-size effects [where $D_{tr}(\text{TCP})$ scales inversely with pore length in the pore center], and also to incorporate pore end effects [noting that $D_{tr}(\text{TCP})$ is enhanced near pore openings] [11,23,30,31]. Incorporating D_{tr} with these features into analysis of catalytic conversion with inhibited diffusion in finite nanopores (including the case of SFD) has been shown to recover precisely all features of behavior in these processes [11,23].

Finally, it is also natural to use (14) to motivate the definition generalized tracer diffusion coefficients for our SFD model with *unequal hop rates* in terms of fluxes obtained from a TCP-type analysis via

$$\begin{aligned} D_{tr}(A|\text{TCP}) &\equiv -J_A/\nabla\langle A \rangle \quad \text{and} \\ D_{tr}(B|\text{TCP}) &\equiv -J_B/\nabla\langle B \rangle \quad (\text{for } h_A \neq h_B). \end{aligned} \quad (15)$$

Extended TCP analysis in Sec. IV will use these definitions to extract generalized tracer diffusion coefficients. More precisely, $D_{tr}(A, B|\text{TCP})$ are obtained from a spatially discrete analog of (15) where $\nabla\langle C \rangle$ is obtained from $(\langle C_n \rangle - \langle C_{n-1} \rangle)/a$. From the relation (4) in Sec. II, it is clear that

$$D_{tr}(A|\text{TCP})/D_{tr}(B|\text{TCP}) = h_A/h_B = D_0(A)/D_0(B). \quad (16)$$

IV. EXTENDED TCP ANALYSIS: KINETIC MONTE CARLO SIMULATION RESULTS

In this section, we report the results for $D_{tr}(A|\text{TCP})/(a^2 h_A) = D_{tr}(B|\text{TCP})/(a^2 h_B)$, denoted by $D_{tr}(\text{TCP})/(a^2 h)$ for convenience, from kinetic Monte Carlo (KMC) simulation studies of standard and extended TCP analysis of our two-component LG model with SFD. Generally, we consider unequal hop rates $h_A \neq h_B$. We select a pore length of $L = 50$ cells or sites, and a total concentration in both coupled reservoirs of $\langle X \rangle$ ranging from 0.1 to 0.9. We consider ratios of hop rates $h_A/h_B = 1$, $h_A/h_B = 5$ and $h_A/h_B = 50$. Results for $h_A/h_B = 1$ are available in Refs. [30,31]. Naturally, any effects of unequal mobility of the two components will be most clear for $h_A/h_B = 50$. Our analysis involves running a single long simulation trial averaging behavior over time (after an initial transient period) for each parameter choice in order to obtain precise values

for quantities such as $\langle A_n \rangle$, $\langle B_n \rangle$, and fluxes through the pore.

First, we review results of standard and extended TCP analysis for $h_A/h_B = 1$. Previous standard TCP analysis characterized in detail $D_{tr}(A|\text{TCP}) = D_{tr}(B|\text{TCP}) = D_{tr}(\text{TCP})$ for $h_A/h_B = 1$ [30,31]. These position-dependent quantities are symmetric about the pore center, as follows from the symmetry of the model. They exhibit a plateau in the pore center where [26] $D_{tr}(\text{TCP}) \approx D_0(1 - \langle X \rangle)/[\langle X \rangle(L - 1)]$ and are enhanced near the pore openings. From the linearity of the master equations, and also the boundary conditions at pore openings, it can be shown that for equal mobility, the standard TCP results for $D_{tr}(A|\text{TCP}) = D_{tr}(B|\text{TCP})$ are preserved in an extended TCP analysis where the reservoirs include different mixtures of A and B, but retain the same $\langle X \rangle$ [31].

Next, consider a standard TCP analysis for an extreme case of highly unequal mobility, $h_A/h_B = 50$. Results are shown in Fig. 2 for both the steady-state concentration profiles across the pore, as well as for the corresponding generalized tracer diffusion coefficients. General features seen for $h_A/h_B = 1$ (a plateau in the pore center at least for larger $\langle X \rangle$, and enhanced values near pore openings) are preserved. However, a clear asymmetry about the pore center is evident, particularly for lower $\langle X \rangle$. Specifically, $D_{tr}(\text{TCP})/(a^2 h)$ is greater near the left end of the pore attached to the reservoir of A rather than B. This is particularly clear even for higher $\langle X \rangle$ in the regions where $D_{tr}(\text{TCP})$ is enhanced near the pore openings. This feature is perhaps not surprising since A is the more mobile species, and its population dominates that of slower species near the left end of the pore.

A shortcoming of the above analysis for $D_{tr}(\text{TCP})/(a^2 h)$ is that it convolutes behavior for different mixtures of A and B for a specific total concentration $\langle X \rangle$. Ideally, one would want to determine $D_{tr}(\text{TCP})/(a^2 h)$ for specific individual concentrations, $\langle A \rangle$ and $\langle B \rangle$, as well as for specific $\langle X \rangle = \langle A \rangle + \langle B \rangle$.

This is achieved by an extended TCP analysis. First, we analyze the case where $\langle A \rangle = \langle B \rangle = \langle X \rangle/2$. To this end we perform a sequence of simulations where the concentration of A [B] in the left reservoir is $r\langle X \rangle [(1-r)\langle X \rangle]$, and the concentration of A [B] in the right reservoir is $(1-r)\langle X \rangle [r\langle X \rangle]$. Thus, $r = 1$ corresponds to standard TCP, but we analyze behavior for the sequence of values $r = 0.8, 0.7, 0.6, 0.55, 0.52$ approaching $r = \frac{1}{2}$, where $r = \frac{1}{2}$ corresponds to exactly equal concentrations of A and B in the pore. As $r \rightarrow \frac{1}{2}$, the difference in concentrations in the two reservoirs vanishes, and thus the fluxes, J_A and J_B , also vanish. The closer r is to $\frac{1}{2}$, the smaller the fluxes and the more difficult it is to obtain precise values of desired quantities (given fluctuations in the stochastic model). Thus, $r = 0.52$ is a compromise between reliable statistics and uniform concentrations. By considering behavior for the above sequence of r values we can assess the degree of convergence as $r \rightarrow \frac{1}{2}$.

Results for $D_{tr}(\text{TCP})/(a^2 h)$ are shown in Fig. 3 for $h_A/h_B = 5$ (for which precise results are more readily obtained than for $h_A/h_B = 50$), for a range of different values of $\langle X \rangle$. For $h_A/h_B = 5$ and $\langle A \rangle = \langle B \rangle = \langle X \rangle/2$ with $L = 50$ as r decreases toward $\frac{1}{2}$, $D_{tr}(\text{TCP})/(a^2 h)$ converges to a form symmetric about the pore center for all $\langle X \rangle$. The minimum values realized in the pore center are $D_{tr}(\text{TCP min})/(a^2 h) = 0.176, 0.0226, 0.0133, \text{ and } 0.00098$,

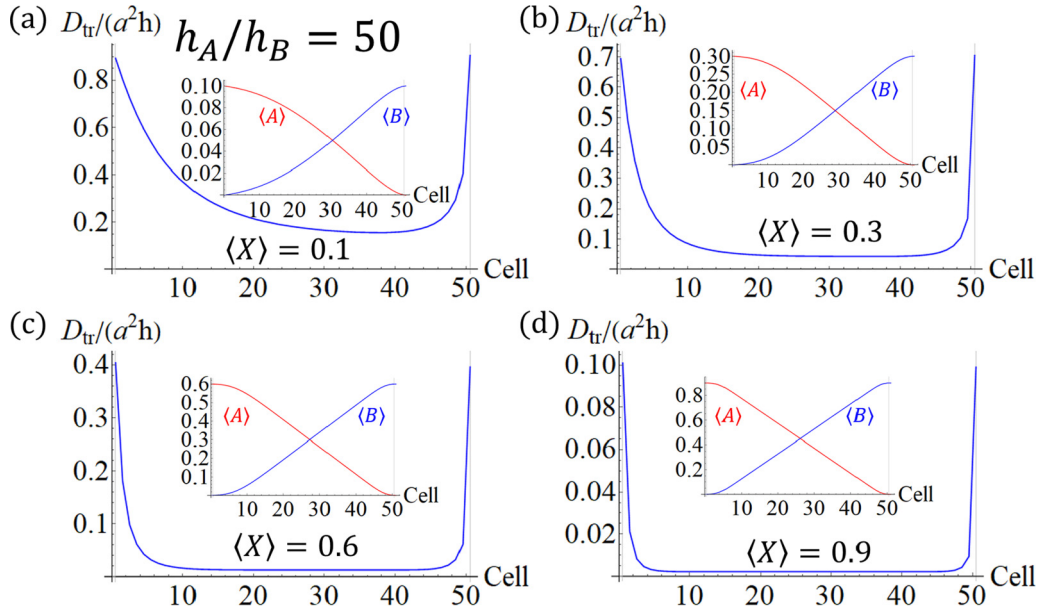


FIG. 2. Standard TCP analysis of the generalized tracer diffusion coefficient D_{tr} for a pore with $L = 50$ for $\langle X \rangle = 0.1$ (a), 0.3 (b), 0.6 (c), and 0.9 (d), and with $h_A/h_B = 50$ in all cases. D_{tr} is strongly enhanced approaching the pore openings. The insets show the concentration profiles from which D_{tr} was extracted highlighting the feature that these D_{tr} are associated with strongly varying partial concentrations of A and B.

for $\langle X \rangle = 0.1, 0.3, 0.6,$ and 0.9 , respectively. The strong dependence on $\langle X \rangle$ is reminiscent of but not identical to that for $h_A = h_B$.

Finally, we further extend our TCP procedure to consider the dependence of $D_{tr}(\text{TCP})/(a^2h)$ on the relative concentrations of $\langle A \rangle$ and $\langle B \rangle$ for fixed total $\langle X \rangle = 0.3$, just considering the case $h_A/h_B = 5$. The above analysis assessed behavior for $\langle A \rangle = \langle B \rangle = 0.15$. Here, instead, we first assess behavior for $\langle A \rangle = 0.21$ and $\langle B \rangle = 0.09$, i.e., a dominant

population of more mobile species. To this end, one performs a sequence of simulations where the concentration of A [B] in the left reservoir is $0.21 + \delta[0.09 - \delta]$, and the concentration of A [B] in the right reservoir is $0.21 - \delta[0.09 + \delta]$. Results shown in Fig. 4 indicate that $D_{tr}(\text{TCP min})/(a^2h) \approx 0.054$ in the limit of small δ . This should be compared with the value $D_{tr}(\text{TCP min})/(a^2h) = 0.023$ for $\langle A \rangle = \langle B \rangle = 0.15$ (with the same h_A/h_B and $\langle X \rangle$). Thus, as might be expected, $D_{tr}(\text{TCP min})/(a^2h)$ is enhanced upon increasing the

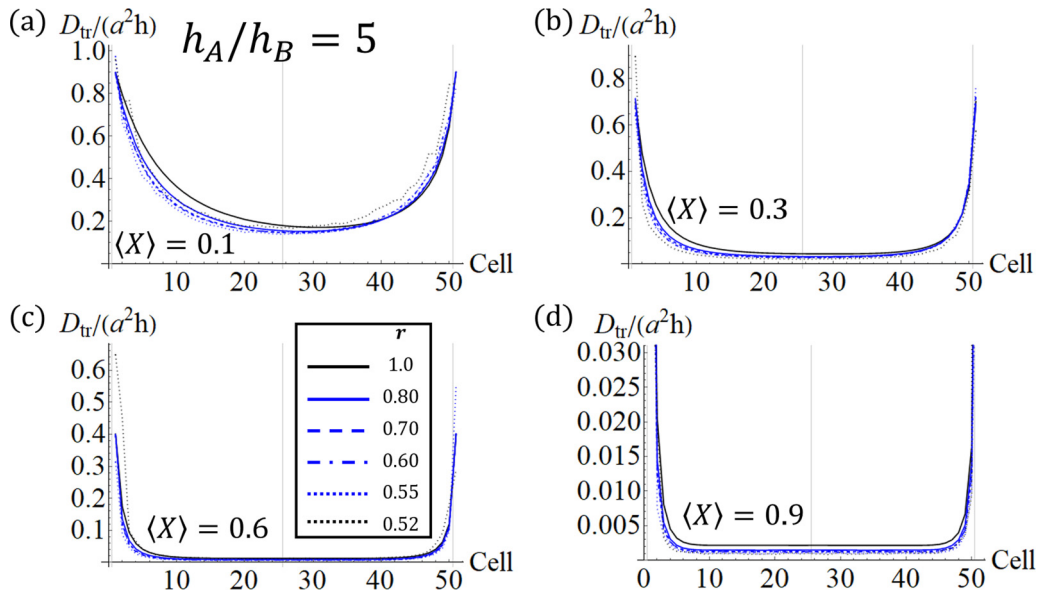


FIG. 3. Extended TCP analysis of the generalized tracer diffusion coefficient D_{tr} in the limit where $\langle A \rangle = \langle B \rangle = \langle X \rangle/2$ for a pore with $L = 50$. Results are shown for $\langle X \rangle = 0.1$ (a), 0.3 (b), 0.6 (c), and 0.9 (d), and with $h_A/h_B = 5$ in all cases. Again, D_{tr} is strongly enhanced approaching the pore openings. In each case, behavior is shown for $r = 1, 0.8, 0.7, 0.6, 0.55,$ and 0.52 , where $r \rightarrow \frac{1}{2}$ corresponds to $\langle A \rangle = \langle B \rangle$ in both reservoirs.

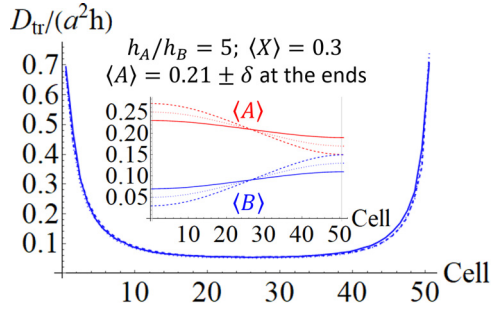


FIG. 4. Extended TCP analysis of the generalized tracer diffusion coefficient D_{tr} for $h_A/h_B = 5$ exploring behavior in the limit where $\langle A \rangle = 0.21$ and $\langle B \rangle = 0.09$ with $L = 50$. Results for $\langle A \rangle = 0.21 \pm \delta$, $\langle B \rangle = 0.09 \mp \delta$ at the pore ends are shown with $\delta = 0.06$ (dotted), 0.04 (dashed), and 0.02 (solid). Again, D_{tr} is strongly enhanced approaching the pore openings. The insets show the concentration profiles from which D_{tr} was extracted for various δ .

proportion of the more mobile species for the same fixed total concentration.

For completeness, it is natural to also analyze behavior for $\langle A \rangle = 0.09$ and $\langle B \rangle = 0.21$, i.e., a dominant population of less mobile species. To this end, we perform a sequence of simulations where the concentration of A [B] in the left reservoir is $0.09 + \delta$ [$0.21 - \delta$], and the concentration of A [B] in the right reservoir is $0.09 - \delta$ [$0.21 + \delta$]. Results shown in Fig. 5 indicate that $D_{\text{tr}}(\text{TCP min})/(a^2 h) \approx 0.019$ in the limit of small δ compared with $D_{\text{tr}}(\text{TCP min})/(a^2 h) = 0.023$ for $\langle A \rangle = \langle B \rangle = 0.15$. Thus, $D_{\text{tr}}(\text{TCP min})/(a^2 h)$ is reduced upon increasing the proportion of the less mobile species.

V. DISCUSSION

A. Tracer diffusion with periodic boundary conditions

It is natural to compare the results of our extended TCP analysis for tracer diffusion in finite open systems with results from more conventional analysis in finite systems with periodic boundary conditions (PBC). For PBC, the tagged particle displacement is defined so as to be able to increase without

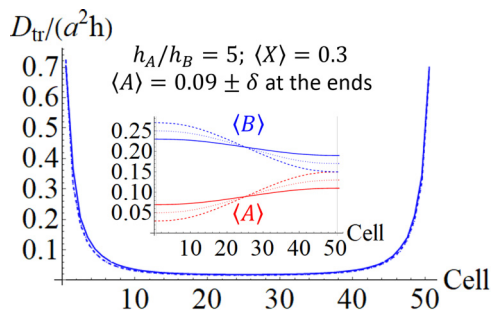


FIG. 5. Extended TCP analysis of the generalized tracer diffusion coefficient D_{tr} for $h_A/h_B = 5$ exploring behavior in the limit where $\langle A \rangle = 0.09$ and $\langle B \rangle = 0.21$ with $L = 50$. Results for $\langle A \rangle = 0.09 \pm \delta$, $\langle B \rangle = 0.21 \mp \delta$ at the pore ends are shown with $\delta = 0.06$ (dotted), 0.04 (dashed), and 0.02 (solid). Again, D_{tr} is strongly enhanced approaching the pore openings. The insets show the concentration profiles from which D_{tr} was extracted for various δ .

bound if the particle cycles through the system arbitrarily many times in the same direction. For our two-component LG model, it is clear that the SFD constraint implies that the mean-square placement of tagged particles of either species has the same long-time asymptotic behavior. Thus, the same tracer diffusion coefficient, $D_{\text{tr}}(\text{PBC})$, applies for both species. For $h_A/h_B = 1$, the tracer diffusion coefficient corresponds to that for a single-component system, where exact analysis shows that [26] $D_{\text{tr}} = D_0(1 - \langle X \rangle)/[\langle X \rangle(L - 1)]$ for $\langle X \rangle = N/L$ with integer total number of particles $1 \leq N \leq L$.

We have performed a comprehensive simulation analysis of $D_{\text{tr}}(\text{PBC})$ for general unequal mobility and general partial concentrations $\langle A \rangle = N_A/L$ and $\langle B \rangle = N_B/L$ where N_A (N_B) denotes the number of A (B). Varying all of h_A/h_B , $\langle A \rangle/\langle B \rangle$, $\langle X \rangle$, and L indicates that

$$D_{\text{tr}}(\text{PBC}) = [x_A/D_0(A) + x_B/D_0(B)]^{-1}(1 - \langle X \rangle)/[\langle X \rangle(L - 1)], \quad (17)$$

where $x_A = \langle A \rangle/\langle X \rangle$ and $x_B = \langle B \rangle/\langle X \rangle$ are fractional species concentrations, so that $x_A + x_B = 1$. Results from simulations supporting this form are provided in the Supplemental Material [37]. The form of (17) is reminiscent of series resistance behavior: $x_A N$ resistors with resistance $R_A = 1/D_0(A)$ in series with $x_B N$ resistors with resistance $R_B = 1/D_0(B)$ have overall resistance $R_{\text{tot}} = (x_A R_A + x_B R_B)N$, and overall conductance inversely proportional to this quantity.

The form of the dependence on partial coverages and diffusivities also reflects that of the exact results (11) for hydrodynamic chemical diffusion coefficients. It thus also recovers intuitive limiting behavior, e.g., $D_{\text{tr}}(\text{PBC}) \sim D_0(B)(1 - \langle X \rangle)/[\langle B \rangle(L - 1)]$, as $D_0(A)/D_0(B) \rightarrow \infty$, which is controlled by the mobility of the slow species. In particular, for a single slow particle B, where $\langle B \rangle = 1/L$, one recovers the simple mean-field result, $D_{\text{tr}}(\text{PBC}) \sim D_0(B)(1 - \langle A \rangle^*)$, as $D_0(A)/D_0(B) \rightarrow \infty$, where $\langle A \rangle^* = N_A/(L - 1)$ is the local concentration of highly mobile A species on sites not occupied by B.

B. PBC versus extended TCP results

It is natural to compare tracer diffusivity values from the TCP analysis with that from the PBC analysis. Here, we consider the case $h_A/h_B = 5$, $\langle X \rangle = 0.3$, and $L = 50$. From (17) for equal concentrations of A and B, $x_A = x_B = \frac{1}{2}$, one has that $D_{\text{tr}}(\text{PBC}) = 0.079(a^2 h_B)$. Extended TCP analysis with the same parameters gave minimum plateau values for tracer diffusivity in the pore center of $D_{\text{tr}}(A|\text{TCP min}) = 0.133(a^2 h_B)$ and $D_{\text{tr}}(B|\text{TCP min}) = 0.027(a^2 h_B)$; i.e., $D_{\text{tr}}(\text{PBC})$ adopts a value intermediate between the TCP values of $D_{\text{tr}}(A, B|\text{TCP min})$. This feature also applies for unequal concentrations of A and B. Results for $x_A = 0.3$ and $x_B = 0.7$ (a dominant population of slow species) and for $x_A = 0.7$ and $x_B = 0.3$ (a dominant population of fast species) are shown in Table I together with those for $x_A = x_B = \frac{1}{2}$. Results show that $D_{\text{tr}}(\text{PBC})$ always lies in between $D_{\text{tr}}(B|\text{TCP min})$ and $D_{\text{tr}}(A|\text{TCP min})$.

It should be emphasized that the analysis of tracer diffusion in closed systems with PBC and in open systems with a TCP-type setup corresponds to fundamentally different

TABLE I. Comparison of minimum values of tracer diffusion coefficients from an extended TCP analysis with that for an analysis with periodic boundary conditions (PBC). In all cases, one has $h_A/h_B = 5$, $\langle X \rangle = 0.3$, and $L = 50$.

$h_A/h_B = 5$	$D_{\text{tr}}(\text{B} \text{TCP min})/(a^2 h_B)$	$D_{\text{tr}}(\text{PBC})/(a^2 h_B)$	$D_{\text{tr}}(\text{A} \text{TCP min})/(a^2 h_B)$
$x_A = 0.3, x_B = 0.7$	0.019	0.063	0.095
$x_A = x_B = 0.5$	0.027	0.079	0.133
$x_A = 0.7, x_B = 0.3$	0.054	0.108	0.270

ensembles: a canonical ensemble for PBC versus a grand canonical ensemble for the TCP-type setup. There is a reasonable correspondence between the PBC result and plateau value of tracer diffusivity in the pore center for the TCP analysis with equal mobility. The situation is more complicated for unequal mobility, as indicated above, with the single tracer diffusion coefficient for both species from analysis with PBC adopting a value in between the two distinct plateau values for different species from the TCP-type analysis.

C. Multicomponent SFD systems

It is natural to extend our analysis for two-component systems to multicomponent systems. For TCP, the two reservoirs connected to opposite ends of the pore would contain different mixtures of the multiple species, A, B, C, etc., with the same total concentration $\langle X \rangle$. One allows for generally different hop rates, h_A, h_B, h_C , etc., for A, B, C, etc. respectively. Extending the exact master equation analysis in Sec. II A, it follows that

$$J_A/h_A + J_B/h_B + J_C/h_C + \dots = 0. \quad (18)$$

One naturally defines tracer diffusion coefficients in terms of fluxes and concentration gradients for the extended TCP setup via $D_{\text{tr}}(\text{A}|\text{TCP}) \equiv -J_A/\nabla\langle A \rangle$, etc., as in (15). One can consider special cases where concentrations of only a pair of species, say, A and B, differ in the two reservoirs (so C, etc., have the same concentration, and consequently $J_C = 0$, etc.). In this special case, once again one recovers the result (16) relating the distinct tracer diffusion coefficients for A and B.

Regarding hydrodynamic theory for noninteracting multicomponent SFD systems, again analysis of compressibilities is straightforward. Also, it is clear that imposing a driving force on any one species induces the same diffusion flux for all species. $\Lambda_{AA} : \Lambda_{BA} : \Lambda_{CA} : \dots = \langle A \rangle : \langle B \rangle : \langle C \rangle : \dots$, etc., leading to extension of the analysis for the two-component case. Regarding the analysis of tracer diffusivity in finite systems with periodic boundary conditions, it is again the case that the SFD condition implies the same tracer diffusion coefficient, $D_{\text{tr}}(\text{PBC})$, for all species. Insight into the behavior of this diffusion coefficient is also reasonably achieved through a mixed series resistor analogy, as in the two-component case.

VI. CONCLUSIONS

Our extended TCP analysis has provided detailed insight into tracer diffusion coefficients for the two-component SFD system in a finite open nanopore with generally unequal mobility of the two components. In particular, this formalism opens the possibility to quantify tracer diffusivity for specific selected concentrations of the two components, and thus to systematically assess the variation in behavior upon varying

the total concentration or the relative concentrations of the components. The tracer diffusion coefficients extracted from the extended TCP analysis should be regarded as generalized hydrodynamic diffusion coefficients as they apply for finite systems, and thus do not vanish as is the case for tracer diffusivity for any infinite SFD system. Significantly, while these diffusion coefficients have a well-defined plateau value in the pore center (provided the pore is sufficiently long), their values are always significantly enhanced near the pore openings. One might regard stochastic adsorption-desorption processes at the pore openings as offsetting the SFD constraint in the regions near the pore openings, and thus enhancing tracer diffusivity. It should be noted that even higher-level analytic dynamic mean-field-type analysis of tracer diffusivity, which applies truncation approximations to the exact hierarchical master equations, fails to quantitatively capture behavior. See the Appendix and the Supplemental Material [37]. This is due to the generation of strong nonequilibrium spatial correlations as a result of the SFD constraint [11,36].

It is also appropriate to emphasize that enhancement of tracer diffusivity near pore openings is expected to be critical in controlling concentration distributions within the pore, and thus reactivity, for systems where SFD within the pore is coupled to a conversion reaction within the pore. This feature has been previously confirmed from the case of equal mobility of reactants and products in such a SFD system [11,23].

ACKNOWLEDGMENTS

This work was supported by the U.S. Department of Energy (USDOE), Office of Basic Energy Sciences, Division of Chemical Sciences, Geosciences, and Biosciences through the Ames Laboratory Chemical Physics program. The work was performed at Ames Laboratory which is operated for the USDOE by Iowa State University under Contract No. DE-AC02-07CH11358.

APPENDIX: APPROXIMATE HIERARCHICAL TRUNCATION ANALYSIS

An analytic treatment of TCP-type problems involves analysis of the appropriate heterogeneous hierarchical master equations, the lowest-order example of which is given by (1) with expressions for the diffusion fluxes given in (2). In addition, appropriate boundary conditions at the pore ends must be applied. As noted in the text, there exist different levels of hierarchical truncation approximation of these equations which we describe explicitly below. It is natural to compare the predictions of these different approximations with precise KMC simulation results for tracer diffusion coefficients.

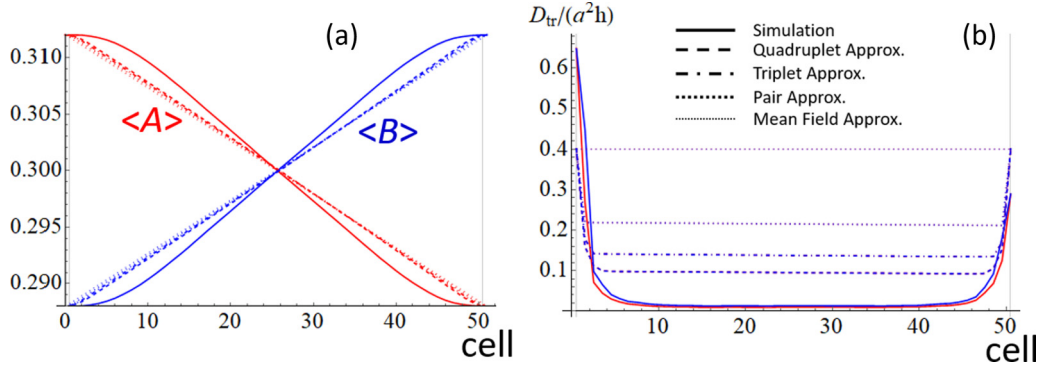


FIG. 6. Results from an extended TCP analysis for $h_A/h_B = 5$, $\langle X \rangle = 0.6$, and $L = 50$ for $D_{tr}(\text{TCP})/(a^2h)$ from site through quartet approximations compared with KMC simulation.

The lowest-order mean-field or site approximation ignores all spatial correlations, and thus factorizes $\langle A_n E_{n+1} \rangle = \langle A_n \rangle \langle E_{n+1} \rangle$, $\langle E_n A_{n+1} \rangle = \langle E_n \rangle \langle A_{n+1} \rangle$, etc., where $\langle E_n \rangle = 1 - \langle X_n \rangle = 1 - \langle X \rangle$ for our TCP setup. It immediately follows that, e.g.,

$$J_A = h_A(1 - \langle X \rangle) \nabla \langle A_n \rangle, \quad \text{so that} \\ D_{tr}(A|\text{TCP}) = a^2 h_A (1 - \langle X \rangle), \quad (\text{A1})$$

$$\begin{aligned} \langle F_n G_{n+1} H_{n+2} \rangle &= \langle F_n G_{n+1} \rangle \langle G_{n+1} H_{n+2} \rangle / \langle G_{n+1} \rangle \quad (\text{pair}), \\ \langle F_n G_{n+1} H_{n+2} J_{n+3} \rangle &= \langle F_n G_{n+1} H_{n+2} \rangle \langle G_{n+1} H_{n+2} J_{n+3} \rangle / \langle G_{n+1} H_{n+2} \rangle \quad (\text{triplet}), \\ \langle F_n G_{n+1} H_{n+2} J_{n+3} K_{n+4} \rangle &= \langle F_n G_{n+1} H_{n+2} J_{n+3} \rangle \langle G_{n+1} H_{n+2} J_{n+3} K_{n+4} \rangle / \langle G_{n+1} H_{n+2} J_{n+3} \rangle \quad (\text{quartet}), \\ &\text{etc.} \end{aligned} \quad (\text{A2})$$

Implementation of the pair approximation requires simultaneous analysis of Eq. (1) for single-site probabilities as well as additional equations for pair probabilities (which together form a closed set). The triplet approximation requires simultaneous analysis of equations for single-site, pair, and triplet probabilities, etc.

Next, we present results from application of these approximations to analyze TCP systems for a two-component SFD system in a finite open nanopore with $L = 50$. We compare these predictions against precise KMC simulation results. Here, we show only results from an *extended TCP analysis*, but additional results for a standard TCP analysis are shown in the Supplemental Material [37]. In contrast to

which constitutes a severe overestimate of the actual value of $D_{tr}(A|\text{TCP})$.

Let F, G, H, K, L, ... denote any of A, B, or E. Then, successively higher-level pair, triplet, quartet, etc., approximations utilize the following factorizations of multisite probabilities [11]:

KMC simulation, it is appropriate to note that there is no practical limitation in choosing a very slight difference in concentrations of each species between the two reservoirs at opposite ends of the pore. Thus, one can choose r (defined in the main text) to be extremely close to 0.5. However, for consistency and for comparison with results in the main text, here we choose $r = 0.52$. In Fig. 6, we show results for concentration profiles and tracer diffusivity for $h_A/h_B = 5$, $\langle X \rangle = 0.6$, $L = 50$, and $r = 0.52$. The truncation approximations show the correct trend for increasing truncation order with results for D_{tr} approaching precise simulation values. However, the few lowest-order approximations are far from quantitatively precise.

- [1] A. L. Hodgkin and R. D. Keynes, *J. Physiol. (London, UK)* **128**, 61 (1955).
- [2] E. J. Harris, *Transport and Accumulation in Biological Systems* (Academic Press, London, 1960).
- [3] E. J. A. Lea, *J. Theor. Biol.* **5**, 102 (1963).
- [4] J. Kim, L.-C. Lin, R. L. Martin, J. A. Swisher, M. Haranczyk, and B. Smit, *Langmuir* **28**, 11914 (2012).
- [5] P. Bai, M.Y. Jeon, L. Ren, C. Knight, M.W. Deem, M. Tsapatsis, and J.I. Siepmann, *Nat. Commun.* **6**, 5912 (2015).

- [6] P. J. Bereciartua, A. Cantín, A. Corma, J. L. Jordá, M. Palomino, F. Rey, S. Valencia, E. W. Corcoran, P. Kortunov, P. I. Ravikovitch, A. Burton, C. Yoon, Y. Wang, C. Paur, J. Guzman, A. R. Bishop, and G. L. Casty, *Science* **358**, 1068 (2017).
- [7] A. Siria, M. L. Bocquet, and L. Bocquet, *Nat. Rev. Chem.* **1**, 0091 (2017).
- [8] *Catalysis and Adsorption in Zeolites*, edited by G. Ohlmann, H. Pfeifer, and G. Fricke (Elsevier, Amsterdam, 1991).

- [9] N. Y. Chen, J. T. F. Degnan, and C. M. Smith, *Molecular Transport and Reaction in Zeolites* (Wiley-VCH, New York, 1994).
- [10] J. Kärger, in *Handbook on Heterogenous Catalysis*, edited by G. Ertl, H. Knözinger, F. Schüth, and J. Weitkamp (Wiley-VCH, Weinheim, 2008), p. 1714.
- [11] D.-J. Liu, A. García, J. Wang, D. M. Ackerman, C.-J. Wang, and J. W. Evans, *Chem. Rev.* **115**, 5979 (2015).
- [12] T. E. Harris, *J. Appl. Probab.* **2**, 323 (1965).
- [13] F. Marchesoni and A. Taloni, *Phys. Rev. Lett.* **97**, 106101 (2006).
- [14] L. Lizana and T. Ambjörnsson, *Phys. Rev. Lett.* **100**, 200601 (2008).
- [15] P. L. Krapivsky, K. Mallick, and T. Sadhu, *Phys. Rev. Lett.* **113**, 078101 (2014).
- [16] H. Spohn, *Large Scale Dynamics of Interacting Particles* (Springer, Berlin, 1991).
- [17] A. Massi and E. Presutti, *Mathematical Methods for Hydrodynamic Limits*, Springer Lecture Notes in Mathematics Vol. 1501 (Springer, Berlin, 1991).
- [18] J. W. Evans, D.-J. Liu, and M. Tammaro, *Chaos* **12**, 131 (2002).
- [19] D.-J. Liu and J. W. Evans, *Prog. Surf. Sci.* **88**, 393 (2013).
- [20] C. Rodenbeck, J. Karger, and K. Hahn, *J. Catal.* **157**, 656 (1995).
- [21] M. S. Okino, R. Q. Snurr, H. H. Kung, J. E. Ochs, and M. L. Mavrouniotis, *J. Chem. Phys.* **111**, 2210 (1999).
- [22] S. V. Nedeá, A. P. J. Jansen, J. J. Lukkien, and P. A. J. Hilbers, *Phys. Rev. E* **65**, 066701 (2002).
- [23] D. M. Ackerman, J. Wang, and J. W. Evans, *Phys. Rev. Lett.* **108**, 228301 (2012).
- [24] B. J. Alder and W. E. Alley, *Phys. Today* **37**(1), 56 (1984).
- [25] L. Onsager, *Phys. Rev.* **37**, 405 (1931).
- [26] H. van Beijeren, K. W. Kehr, and R. Kutner, *Phys. Rev. B* **28**, 5711 (1983).
- [27] D. G. Levitt and G. Subramanian, *Biochim. Biophys. Acta* **373**, 132 (1974).
- [28] H. Hahn and J. Kärger, *J. Phys. Chem. B* **102**, 5766 (1998).
- [29] P. H. Nelson and S. M. Auerbach, *J. Chem. Phys.* **110**, 9235 (1999).
- [30] P. H. Nelson and S. M. Auerbach, *Chem. Eng. J.* **74**, 43 (1999).
- [31] D. M. Ackerman and J. W. Evans, *Phys. Rev. E* **95**, 012132 (2017).
- [32] R. Kutner, *Phys. Lett. A* **81**, 239 (1981).
- [33] J. Quastel, *Commun. Pure Appl. Math.* **45**, 623 (1992).
- [34] H. E. Stanley, *Introduction to Phase Transitions and Critical Phenomena* (Oxford University Press, Oxford, 1971).
- [35] J. W. Evans, P. A. Thiel, and M. C. Bartelt, *Surf. Sci. Rep.* **61**, 1 (2006).
- [36] A. García, J. Wang, T. L. Windus, A. D. Sadow, and J. W. Evans, *Phys. Rev. E* **93**, 052137 (2016).
- [37] See Supplemental Material at <http://link.aps.org/supplemental/10.1103/PhysRevE.101.062103> for additional results for tracer diffusivity $D_{tr}(TCP)/(a^2h)$ from hierarchical truncation approximation of the exact heterogeneous master equations and results for tracer diffusivity $D_{tr}(PBC)$ from KMC simulation.
- [38] H. van Beijeren and K.W. Kehr, *J. Phys. C: Solid State Phys.* **19**, 131 (1986).
- [39] K. W. Kehr, K. Binder, and S. M. Reulein, *Phys. Rev. B* **39**, 4891 (1989).